Current Applied Physics 15 (2015) 1107–1110

Contents lists available at ScienceDirect

Current Applied Physics

journal homepage: www.elsevier.com/locate/cap

Quantum size effect of surface-channeled charge carrier transport in Au nanoparticles-VO_2 nanowire assembly

Gil-Ho Kim [a], Servin Rathi [a], Jeong Min Baik [b], Kyung Soo Yi [c, *]

[a] School of Electronic and Electrical Engineering and Sungkyunkwan Advanced Institute of Nanotechnology (SAINT), Sungkyunkwan University, Suwon 440-746, Republic of Korea
[b] School of Mechanical and Advanced Materials Engineering, UNIST, Ulsan 689-805, Republic of Korea
[c] Department of Physics, Pusan National University, Busan 609-735, Republic of Korea

ARTICLE INFO

Article history:
Received 2 June 2015
Received in revised form
11 June 2015
Accepted 18 June 2015
Available online 20 June 2015

Keywords:
Quantum size effect
VO_2 nanowire assembly
Nanojunction
Subband structure

ABSTRACT

Confined charge carriers in nano-scaled structures have revealed great impacts on scientific and technological advances during the last few decades. Here we present quantum size effect of surface-channeled Au nanoparticles-VO_2 nanowire assembly fabricated via ac dielectrophoresis. Carrier injection is manipulated through Au nanoparticles decorated on the surface of single crystal VO_2 nanowire. Plateau structures are seen in the I–V characteristic of the assembly at 150 K, and the corresponding oscillation in channel conductance is analyzed in terms of quantum confinement induced two-dimensional layer of the carriers in a nanobelt formed around the insulating core of the VO_2 nanowire.

1. Introduction

The number of charge carriers is a basic quantity in controlling material properties and operation capability. Since the observation of thermally driven insulator-to-metal transition (IMT) in vanadium dioxide (VO_2) [1], this strongly correlated material has attracted much attention over the past decades, because not only of academic curiosities over the puzzling origin of the IMT [2–4] but also its potential application as an energy material of thermochromics, sensors, and switching devices [5,6]. The origin of the mechanism of the IMT in VO_2 is still under debate. The IMT temperature can be varied over a wide range by carrier doping or electron injection via metallic nanoparticles (NPs) deposited on VO_2 nanowire (NW) [7–10] while method of dielectrophoresis (DEP) allows effective manipulation of NPs in a nano-scale environment [11–13]. Recently, it is demonstrated that, with a use of DEP, gold NPs placed on the surface of insulating VO_2 NW donate local charge carriers in the NW and the conductance of the NW could be manipulated in a controlled manner [14]. Carrier conduction was shown to occur through the effectively two-dimensional (2D) surface channel around the insulating core of the NW.

The transport behavior of a channel is sensitive to the relative location of the Fermi levels of the source and drain electrodes, and in the presence of source-drain channel bias V_{sd}, the source and drain Fermi levels can, respectively, be denoted by E_F and $E_F - qV_{sd}$. While the location of the Fermi level in the conduction subband can be tuned with gate bias V_G, the source-drain bias also has a self-gating effect influencing the confinement potential $V(z)$, and, hence, V_{sd} shifts the Fermi levels at the electrodes and induces a current to flow through the channel. At finite temperature, a current can flow only when the subband states are located within a few k_BT around the Fermi levels. As additional subband channels are opened, the current would show stair-like increase until V_{sd} pulls down the drain-side Fermi level below the lowest subband bottom energy. Quantum confinement effect (QCE) is expected to be noticeable in structures of nanoscale. Two conditions must be met to observe quantum oscillations of subband spectroscopy: i) the electronic subbands are well separated and ii) the temperature must be low enough such that the intersubband separations well beat the thermal broadening (~$k_BT \approx$ 12.5 meV at 150 K and 25 meV at 300 K, respectively).

In this work, we demonstrate transport analysis of surface-channeled Au NPs-VO_2 NW assembly fabricated using an ac DEP

* Corresponding author.
E-mail address: ksyi@pusan.ac.kr (K.S. Yi).

http://dx.doi.org/10.1016/j.cap.2015.06.010
1567-1739/

experiment. We interpret the step-like structure, in terms of the QCE, revealed at 150 K in the *I*–*V* characteristic of a VO_2 nano-wire coated with metallic nano-particles employing a simple, quantum mechanical analysis of subband spectroscopy that gives insight in the nature of QCE. Clear plateau structure in the source-drain *I*–*V* curve is revealed at 150 K, and the oscillation in the differential conductance is understood in terms of quantum confinement induced subband structure formation. These quantum size effects are not seen at 300 K (results are reported in Ref. [14]), and the present work is a follow up study of our recent work [14].

2. Experimental

VO_2 [100] NWs of monoclinic structure were grown by physical vapor deposition in a quartz tube furnace under atmospheric pressure from V_2O_5 thin film, which was deposited onto a thermally grown SiO_2 layer of 200 nm thickness on a Si(100) single crystal substrate [15]. Fig. 1(a) shows a schematic overview of the experimental setup for Au NPs-VO_2 NW assembly. For current–voltage probes, the NW was positioned between coplanar Ohmic Ti/Au electrodes (of 4 μm gap) patterned by standard e-beam metal vapor deposition method [6]. VO_2 NW was immersed in distilled water, and Au NPs were suspended to float in the space around the NW. Details of the sample preparation and measurements are reported in Ref. [14]. Au NPs of 10 nm radius were positioned on the surface of VO_2 [100] NW of rectangular cross section (210 nm × 120 nm) and 4 μm length. The number of carriers in the VO_2 NW channel was manipulated with control of the number of adsorbed Au NPs by varying duration and ac voltage of the DEP processing [14,16]. In Fig. 1(b) and (c), scanning electron microscopy (SEM) images are shown for DEP processed Au NPs-VO_2 NW assembly manipulated at 1 MHz and 2.5 V (b) with DEP duration t = 30 s and surface density of Au NPs of 3.51×10^{10} cm^{-2} and (c) with t = 60 s and Au NPs of 1.68×10^{11} cm^{-2}, respectively. The dc *I*–*V* characteristics of the NW were measured using lock-in amplifier with the source and drain electrodes of the VO_2 NW channel placed on top of the SiO_2/Si base substrate. Au NPs were sitting on the three faces of the VO_2 NW.

3. Electrical transport analyses

Transport behavior of a device is sensitive to the relative location of the Fermi levels of the source and drain electrodes, and the location of the Fermi level can be tuned either with gate bias V_G or with source-drain channel bias V_{sd}. The channel bias V_{sd} modulates confinement potential *V*(z) through a self-gating effect influencing the Fermi level at the source and drain electrodes up and down. In the present work, the transport behavior was studied as a function of channel bias and analyzed the confinement effect on the transport behavior.

The current–voltage measurements were carried out in a two-terminal configuration [14]. Fig. 2(a) shows *I*–*V* characteristics at 150 K as a function of source-drain voltage for three different values of Au NP density on the VO_2 NW. The behavior of *I*–*V* and the corresponding channel conductance are illustrated in Fig. 2(b) and (c) for the case of surface concentration 2.91×10^{10} cm^{-2} of Au NPs. The nonlinear symmetric *I*–*V* behavior is a signature of space-charge-limited (SCL) transport [14,17,18], which is more noticeable for higher concentration of Au NPs. We conjecture that the surface confinement potential is strongly dependent on the number of charge carriers in the surface channel and, as the degree of carrier doping is increased in the VO_2 NW, the quadratic SCL behavior overcomes the linear Ohmic contribution and dominates the channel transport at increased biases. Weak hysteretic memory behavior is also observed, as indicated in Fig. 2(a), which offers a

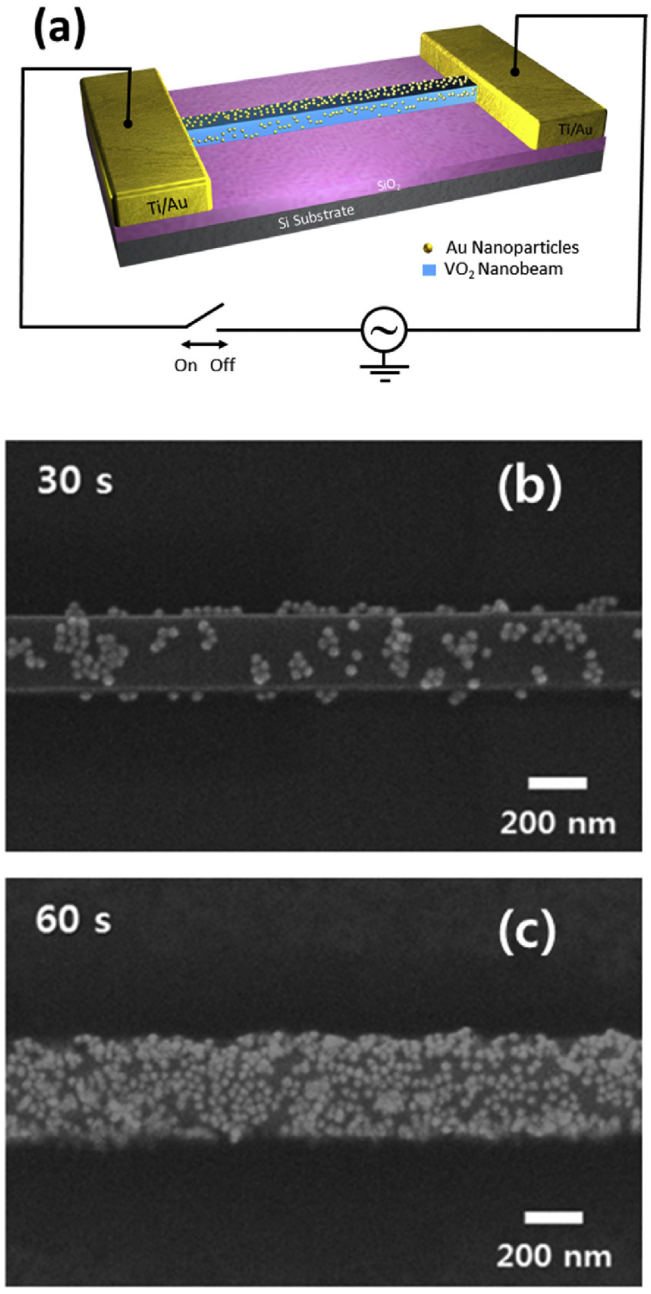

Fig. 1. (a) Schematic overview of experimental setup for Au NPs-VO_2 NW assembly, and scanning electron microscopy (SEM) images of DEP processed Au NPs-VO_2 NW assembly manipulated at 1 MHz and 2.5 V for DEP duration (b) t = 30 s and surface density of Au NPs of 3.51×10^{10} cm^{-2} and (c) t = 60 s and Au NPs of 1.68×10^{11} cm^{-2}.

potential application of the assembly in non-volatile memory devices [19,20]. The electrical transport of the surface-coated insulating VO_2 NW was successfully modeled at 300 K in terms of surface charge carriers (donated by the surface-deposited metallic NPs) and forming surface channels inside the insulating VO_2 NW [14]. The Au NPs dopants provide confining surface potential *V*(z) inside the NW, and the motion of charge carriers is restricted in the direction normal to the surface, hence, creating a channel of quasi-2 dimensional electron gas. We observe symmetric *I*–*V* characteristic and conductance oscillations with period $\Delta V \cong 20$ mV at 150 K. We understand that the decorated Au NPs act as dopant material on the NW surface to give rise to itinerant carriers to insulating VO_2 NW

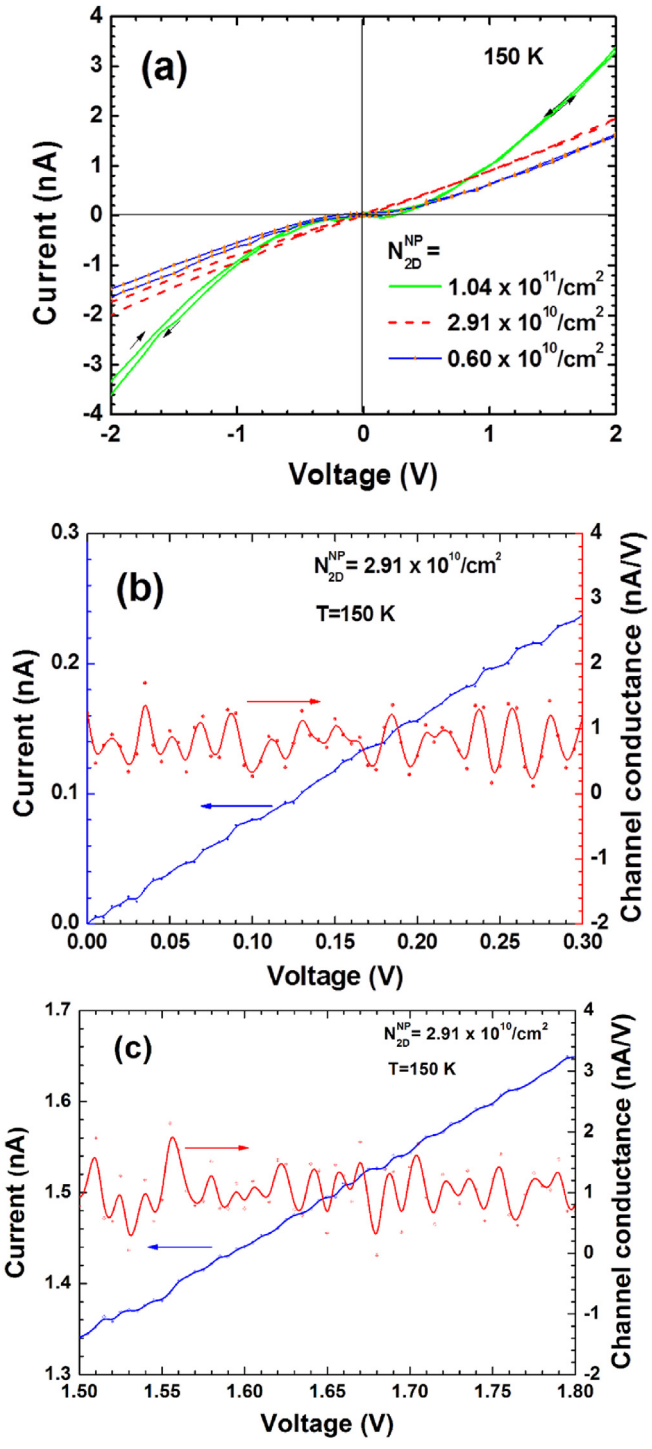

Fig. 2. *I–V* characteristic and the corresponding channel conductance behavior as a function of source-drain voltage for the VO_2 NW at 150 K. *I–V* characteristics at four different Au NP densities (a), *I–V* and the corresponding differential conductance behavior for the Au NPs surface concentration of 2.91 × 10^{10} cm^{-2} in the channel bias voltage regions of (b) V_{sd} = 0–0.3 V, and (c) V_{sd} = 1.5–1.8 V.

and that a thin accumulation layer of electrons is formed around the NW [8,21]. Under an external bias field, the carrier conduction occurs through thus-formed 2D layer of carriers around the insulating core of the VO_2 NW [14]. The cross sectional area of the NW contributing to charge conduction would be reduced much from the physical cross section of the NW.

Observed plateau structures in the *I–V* curve and the oscillations in the channel conductance are analyzed in terms of quantum confinement-induced 2D subband structure of the NW [22]. The source-drain current I is controlled by the potential V between the source and drain electrodes. As the value of channel bias V is increased, higher lying subband states are successively occupied by carriers and additional conduction channels are opened in the device [23]. The surface trapped Au NPs are treated as donors to provide constant electric field E within the NW giving rise to confined charge carriers in a linear potential well inside the NW surface.

One can estimate an order-of-magnitude of the subband structure in an Au NPs-VO_2 NW assembly by treating the surface channel formed around the VO_2 NW as a 2D nanobelt of electrons confined in a one-dimensional surface potential, $V(z)$. The effective potential felt by an electron can be determined by imposing standard boundary conditions on the continuity of the electric potential and the displacement field at the interface of the NW and the outside vacuum [22]. In our analysis we ignore the possible intrinsic carriers presenting in raw VO_2 NWs, and assume all the carriers are injected from the Au NPs. We model that the effective 2D concentration of charged Au atoms and of Au NPs are related by $N_{2D}^{Au} = \alpha N_{2D}^{NP}$, where $\alpha \sim 200$ for Au NPs of radius 10 nm. [24] Then, from the Gauss law in electrostatics, the potential energy of an electron (of charge $q = -e$) inside the NW ($z > 0$) is written as $V(z) = e^2 N_{2D}^{Au} z/(2\varepsilon_0 \varepsilon_{NW})$. The corresponding electric field is $E = eN_{2D}^{Au}/(2\varepsilon_0 \varepsilon_{NW})$. Here eN_{2D}^{Au}, ε_0, and ε_{NW} denote the surface charge concentration due to decorated Au NPs, free space permittivity, and dielectric constant of the NW (~36), respectively. The effective mass of an electron in the metallic phase of VO_2 is $m^* = 2.0$ m, where m is the free electron mass [25]. The characteristic length ℓ of the conducting channel thickness is estimated, by setting $eE\ell = \hbar^2/(2m^*\ell^2)$, to be $\ell \sim 1.1$ nm if $\alpha = 200$.

Because the motion of the carriers normal to the interface is restricted by the potential $V(z)$, the states of the effectively 2D electrons are quantized into subband structures, which are determined, with the physical boundary conditions $\psi(0) = 0 = \psi(\infty)$, by [26]

$$-\left[\hbar^2/(2m^*)\right]\psi''(z) + (eEz - \varepsilon)\psi(z) = 0 \quad (1)$$

for $z > 0$. Eq. (1) can be rewritten, in terms of dimensionless variable $\eta = z/\ell - \lambda$, as

$$\left(d^2/d\eta^2 - \eta\right)\psi(\eta) = 0 \quad (2)$$

with new boundary conditions $\psi_{\eta=-\lambda} = 0 = \psi_{\eta=\infty}$. Here λ denotes dimensionless subband bottom energy (in units of $2m^*\varepsilon\ell^2/\hbar^2$) defined by $\varepsilon_n = \hbar^2\lambda_n/(2m^*\ell^2) \approx 16.0\,\lambda_n$ [meV]. Now, one can obtain the subband bottom energies $\{\varepsilon_n\}$ with $n = 0, 1, 2,\ldots$ by introducing dimensionless variable $\eta = z/\ell - \lambda$. The eigenstates satisfying $\psi_{\eta=\infty} = 0$ is given by Airy function $\psi(\eta) = \mathrm{Ai}(\eta)$, which has zeros with $\eta < 0$. Hence, the boundary condition $\psi_{\eta=-\lambda} = 0$ gives us the eigenenergies λ_n, which are the zeros of $\mathrm{Ai}(\eta{=}-\lambda) = 0$. The first few eigenvalues are $\lambda_1 = 2.338$, $\lambda_2 = 4.088$, $\lambda_3 = 5.521,\ldots$ [27] giving rise to $\Delta\lambda = \lambda_{n+1} - \lambda_n = 1.75$ and 1.43 for $n = 1$ and 2. Therefore, subband separations are $\Delta\varepsilon_{n+1,n} = 16.0 \times (\lambda_{n+1} - \lambda_n)$ [meV] leading us to $\Delta\varepsilon_{2,1} \sim 28.0$ [meV], $\Delta\varepsilon_{3,2} \sim 22.9$ [meV]. Resulting 2D subband structure gives rise to a series of stair-like DOS [22,23]. The period of the conductance oscillation in the *I–V* measurement is $\Delta\varepsilon_{n+1,n}^{exp} \sim 20$ [meV] as seen in Fig. 2(b) and (c). The order-of-magnitude estimation of the subband separation is in agreement with experimentally determined period of channel conductance oscillations. More extended analysis of the case $N_{2D}^{NP} = 2.91 \times 10^{10}\mathrm{cm}^{-2}$ in Fig. 2(a) gives us $\Delta V = 19.6 \pm 0.4$ mV for lower values of the source-drain bias V_{sd} = 0–0.8 V, while $\Delta V \approx 15.3$ mV for higher values of

$V_{sd} = 1.5–1.8$ V as shown in Fig. 2(c) [28]. Therefore, we conjecture that the effective surface channel layer thickness is approximately ~1 nm, and the surface charge density is projected to be $\sigma = e\alpha N_{2D}^{Au} \sim 9.31 \times 10^{-7}$ [C/cm^2]. In our analysis, the effects of exchange-correlations among carriers [22] are neglected and the effect of carrier screening is only included through a static dielectric constant ε_{NW} (~36) of VO_2, but the band structure effect is taken into account within the effective mass formulation.

When we analyzed our results at 300 K (shown in Ref. [14]), the stair-like behavior in the I–V characteristic and the corresponding oscillatory behavior in the channel conductance were not seen due to increased thermal broadening. If one wants to be more complete quantitatively, confinement potential $V(z)$ need be determined self-consistently by solving Eq. (1) coupled with the Poisson equation, and the self-consistent analysis would require much further extended efforts. Resulting $V(z)$ would, in general, be a non-linear function of z, the distance from the surface of the VO_2 NW and would flatten for increased values of z inside the NW. Hence, higher lying subbands are more closely spaced than lower lying ones. However, even a simplest approximation of linear confinement potential gives us an insight on the role of quantum size effects.

4. Summary and conclusion

Electrical transport properties of Au nanoparticles-VO_2 nanowire assembly fabricated via ac dielectrophoresis have been measured and analyzed to investigate quantum size effects in electrical transport of the assembly. We showed that nanojunctions of Au NPs-VO_2 NW assembly gave rise to a new 2D system of highly mobile carriers trapped within a nanowire formed around the insulating core of the VO_2 nanowire. In conclusion, the observed plateau structures in $I–V$ curve at 150 K and the corresponding oscillation in channel conductance could be understood as a realization of confinement induced quantum size effect of the carriers in the nanowire.

Acknowledgments

We thank Youngreal Kwak for assistance in DEP processing of the sample. This research was supported by Basic Science Research Program through the National Research Foundation of Korea funded by the Ministry of Education (grant number 201306330002 and grant number 2013R1A2A2A01069023).

References

[1] F.J. Morin, Oxides which show a metal-to-insulator transition at the Neel temperature, Phys. Rev. Lett. 3 (1959) 34–36.
[2] M.M. Qazilbash, M. Brehm, B.-G. Chae, P.-C. Ho, Andreev, B.-J. Kim, S.J. Yun, A.V. Balatsky, M. BMaple, F. Keilmann, H.-T. Kim, D.N. Basov, Mott transition in VO_2 revealed by Infrared spectroscopy and nano-imaging, Science 318 (2007) 1750.
[3] See, for example D.N. Basov, R.D. Averitt, D. Marel, M. Dressel, K. Haule, Electrodynamics of correlated electron materials, Rev. Mod. Phys. 83 (2011) 471–541 (and the references therein).
[4] A. Zimmers, L. Aigouy, M. Mortier, A. Sharoni, S. Wang, K.G. West, J.G. Ramirez, I.K. Schuller, Role of thermal heating on the voltage induced insulator-metal transition in VO_2, Phys. Rev. Lett. 110 (2013) 56601.
[5] S.-Y. Li, G.A. Niklasson, C.G. Granqvist, Thermochromic fenestration with VO_2 -based materials: three challenges and how they can be met, Thin Solid Films 520 (2012) 3823–3828.
[6] J.M. Baik, M.H. Kim, Larson, C.T. Yavuz, G.D. Stucky, A.M. Wodtke, M. Moskovits, Pd-sensitized single vanadium oxide nanowires: highly responsive hydrogen sensing based on the metal-insulator transition, Nano Lett. 9 (2009) 3980–3984.
[7] K. Shibuya, M. Kawasaki, Y. Tokura, Metal-insulator transition in epitaxial $V_{1-x}W_xO_2$ ($0 \leq x \leq 0.33$) thin films, Appl. Phys. Lett. 96 (2010) 022102.
[8] M. Nakano, K. Shibuya, D. Okuyama, T. Hatano, S. Ono, M. Kawasaki, Y. Iwasa, Y. Tokuya, Collective bulk carrier delocalization driven by electrostatic surface charge accumulation, Nature 487 (2012) 459–462.
[9] G. Xu, C.-M. Huang, M. Tazawa, P. Jin, D.-M. Chen, Miao, Electron injection assisted phase transition in a nano-Au-VO_2 junction, Appl. Phys. Lett. 93 (2008) 061911.
[10] K. Liu, D. Fu, J. Cao, J. Suh, K.X. Wang, C. Cheng, D.F. Ogletree, H. Guo, S. Sengupta, A. Khan, C.W. Yeung, S. Salahuddin, M.M. Deshmukh, J. Wu, Dense electron system from gate-controlled surface metal–insulator transition, Nano Lett. 12 (2012) 6272–6277.
[11] T.B. Jones, Electromechanics of Particles, Cambridge University, New York, 1995, p. p 24.
[12] H.A. Pohl, Dielectrophoresis: The Behavior of Neutral Matter in Nonuniform Electric Fields, Cambridge University Press, Cambridge, 1978, pp. 38–47.
[13] K.D. Hermanson, S.O. Lumsdon, J.P. Williams, E.W. Kaler, O.D. Velev, Dielectrophoretic assembly of electrically functional microwires from nanoparticle suspensions, Science 294 (2001) 1082–1086.
[14] G.-H. Kim, Y. Kwak, I. Lee, S. Rathi, J.M. Baik, K.S. Yi, Conductance control in VO_2 nanowires by surface doping with gold nanoparticles, Appl. Mater. Interfaces 6 (2014) 14812–14818.
[15] J.W. Byon, M.-B. Kim, M.H. Kim, S.Y. Kim, S.H. Lee, B.C. Lee, J.M. Baik, Electrothermally induced highly responsive and highly selective vanadium oxide hydrogen sensor based on metal–insulator transition, J. Phys. Chem. C 116 (2012) 226–230. J. M. Baik, M. H. Kim, C. Larson, A. M. Wodtke, M. Moskovits, Nanostructure-Dependent Metal–Insulator Transitions in Vanadium-Oxide Nanowires. J. Phys. Chem. C 112 (2008) 13328–13331.
[16] D. Cheon, S. Kumar, G.-H. Kim, Assembly of gold nanoparticles of different diameters between nanogap electrodes, Appl. Phys. Lett. 96 (2010) 013101.
[17] A. Talin, F. Leonard, B.S. Swartzentruber, X. Wang, S. Hersee, Unusually strong space-charge-limited current in thin wires, Phys. Rev. Lett. 101 (2008) 076802.
[18] G.-F. Yu, W. Pan, M. Yu, W.-P. Han, J.-C. Zhang, H.-D. Zhang, Y.-Z. Long, Electrical conduction mechanism of an individual polypyrrole nanowire at low temperatures, Nanotechnology 26 (2015) 045703.
[19] K. Liu, D. Fu, J. Cao, J. Suh, K.X. Wang, C. Cheng, D.F. Ogletree, H. Guo, S. Sengupta, A. Khan, C.W. Yeung, S. Salahuddin, M.M. Deshmukh, J. Wu, Dense electron system from gate-controlled surface metal–insulator transition, Nano Lett. 12 (2012) 6272–6277.
[20] W. Kim, A. Javey, O. Vermesh, Q. Wang, Y. Li, H. Dai, Hysteresis caused by water molecules in carbon nanotube field-effect transistors, Nano Lett. 3 (2003) 193–198.
[21] G. Xu, C.-M. Huang, M. Tazawa, P. Jin, D.-M. Chen, L. Miao, Electron injection assisted phase transition in a nano-Au-VO_2 junction, Appl. Phys. Lett. 93 (2008) 061911.
[22] T. Ando, A.B. Fowler, F. Stern, Electronic properties of two-dimensional systems, Rev. Mod. Phys. 54 (1982) 437–672.
[23] K.S. Yi, K. Trivedi, H.C. Floresca, H. Yuk, W. Hu, M. Kim, Room-temperature quantum confinement effects in transport properties of ultrathin Si nanowire field-effect transistors, Nano Lett. 11 (2011) 5465–5470 (and the references therein).
[24] Since the atomic mass and density of gold are 196.9 and 19.32 kg/m^3, respectively, the volume and mass of each NP of radius 10 nm are estimated to be 4.2 x 10^{-24} m^3 and 8.1 x 10^{-24} kg. Hence, N2DAu=αN2DNP with $\alpha \approx 208$.
[25] P. U Jepsen, B.M. Fischer, A. Thoman, H. Helm, J.Y. Suh, R. Lopez, R.F. Haglund Jr., Metal-insulator phase transition in a VO_2 thin film observed with terahertz spectroscopy, Phys. Rev. B 74 (2006) 205103.
[26] L.D. Landau, E.M. Lifshitz, Quantum Mechanics (Nonrelativistic Theory), third ed., Pergamon Press, New York, 1977, p. p 75.
[27] S. Flügge, Practical Quantum Mechanics, Springer-Verlag, New York, 1974, p. p103.
[28] For the values of source-drain bias V_{sd} = 1.0 ~ 1.8 V, we get $\Delta V = 15.9 \pm 0.1$ mV.